



Numerical simulation of wave energy converter based on stochastic resonance and variable magnetization

| | |
|-------|--|
| メタデータ | 言語: English 出版者: SAGE Publications 公開日: 2025-06-16 キーワード (Ja): キーワード (En): Energy harvesting, Nonlinear vibration, Wave energy converter 作成者: 佐藤, 孝洋 メールアドレス: 所属: |
| URL | http://hdl.handle.net/10258/0002000350 |

Numerical Simulation of Wave Energy Converter Based on Stochastic Resonance and Variable Magnetization

Takahiro Sato^{a,1}

^a*Graduate School of Engineering, Muroran Institute of Technology,
27-1 Mizumoto-cho, Muroran, 050-8585, Hokkaido, Japan*
ORCID ID: Takahiro Sato, <https://orcid.org/0000-0002-6471-8754>

Abstract. This paper introduces a wave energy converter (WEC) with stochastic resonance and variable magnetization system in order to effectively obtain electric energy from the ocean wave. Because nonlinear oscillation systems generally have wider frequency range in comparison with linear one, the proposed WEC is suitable for the power generation from ocean waves. Moreover, a numerical analysis method is also introduced to evaluate the characteristics of the proposed WEC. From the numerical simulations, it is shown that the proposed WEC has wider operational frequency range and the frequency characteristic can be changed by the field current.

Keywords. Energy harvesting, Nonlinear vibration, Wave energy converter

1. Introduction

To introduce renewable energy resources into the power systems, various electric power generation systems have been being studied [1]. Among them, the ocean energy is one of the promising renewable energies because of its huge energy potential [2]. Hence, various wave energy converters (WECs) have been studied [3]. Linear generator-based WEC is one of the hopeful systems [4], because its structure is relatively simple and thus suitable from the view of maintenance cost. However, the drawback of this WEC is that the electric power can be generated only when the wave cycle is close to the resonant frequency of the generator system. Of course, the ocean wave condition changes moment by moment and is not composed of single frequency. For this reason, the conventional WECs do not show ideal power generation efficiency [5].

In this paper, a nonlinear WEC system based on stochastic resonance is proposed. By introducing nonlinearity to the linear generator-based WECs, it is expected that the operational condition of WEC is widened thanks to the nonlinear oscillation effects, e.g. entrainments [6]. In addition, to control nonlinearity corresponding to the wave condition, the variable magnetization is also introduced. Although these features improve the performance of WECs, a problem is that the linear vibration theory cannot be applicable to evaluate the performance of nonlinear WECs. For this reason, a numerical simulation method for the proposed WEC is also introduced. From the proposed simulation method, it is shown that the proposed WEC has wide operational frequency range.

¹ Corresponding Author: Takahiro Sato, e-mail: t-sato@muroran-it.ac.jp.

2. Numerical Simulation of Nonlinear WEC

2.1. Proposed WEC system

Figure 1 shows the schematic view of the proposed WEC. This WEC consists of two floating bodies, between which nonlinear magnetic force acts with respect to the relative displacement. By carefully designing this magnetic force and kinetic energy of the floating bodies, the potential energy of this system results in the double-well potential. This potential structure is also generally called the stochastic resonance system. It has been shown that the operational frequency range of this system becomes wider in comparison with linear systems [7], [8]. Moreover, in the proposed WEC, field windings are introduced. By changing the field current, the nonlinear magnetic force is modified. Thus, the nonlinearity of the system can be controlled to adapt ocean wave conditions.

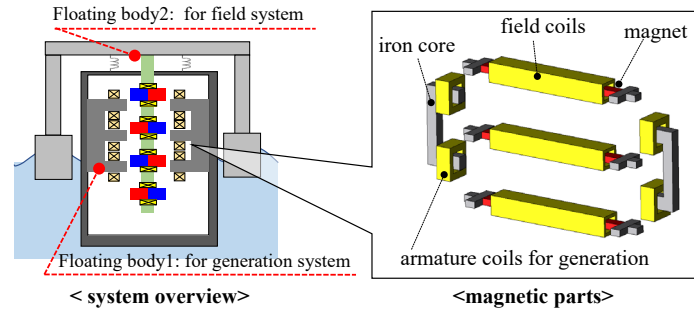


Figure 1. Schematic view of proposed

2.2. Governing equation of proposed WEC

The oscillating behaviors of the two floating bodies can be modeled as 2-DoF spring-mass model, as shown in Fig. 2, by only considering the heave direction. Moreover, we here simply consider repulsion force as the spring, because other hydrodynamic effects do not affect on the nonlinearity, i.e., the potential energy structure. As a result, the governing equations of the proposed WEC system are given as follows:

$$m_1 \ddot{z}_1 + c_1 \dot{z}_1 + c_{12}(\dot{z}_1 - \dot{z}_2) + k_1 z_1 + k_{12}(z_1 - z_2) = f_m(z, I_s, I_f) - m_1 \ddot{y}, \quad (1)$$

$$m_2 \ddot{z}_2 + c_2 \dot{z}_2 + c_{12}(\dot{z}_2 - \dot{z}_1) + k_2 z_2 + k_{12}(z_2 - z_1) = -f_m(z, I_s, I_f) - m_2 \ddot{y}, \quad (2)$$

where $z_1 = x_1 - y$, $z_2 = x_2 - y$, $z = z_1 - z_2$, and y is the base excitation. In addition, I_s and I_f are the armature and field currents, respectively. Moreover, the magnetic force is denoted by f_m . The armature current is governed by the circuit equation based on the loop analysis:

$$\frac{d}{dt} \mathbf{b} \Phi(z, I_s, I_f) + [\mathbf{L}] \frac{d\mathbf{I}}{dt} + [\mathbf{R}] \mathbf{I} = \mathbf{0}, \quad (3)$$

where \mathbf{I} is a loop current vector, $[\mathbf{L}]$ and $[\mathbf{R}]$ are inductance and resistance matrices, respectively. In addition, Φ is the magnetic flux across the armature coil, \mathbf{b} denotes the relation of the armature coil and current loops. To solve these equations, the 2nd-Gear's backward differential formula is employed to discretize in the direction to the time.

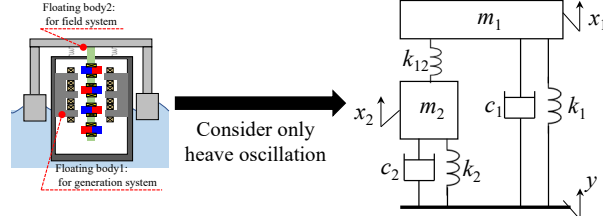


Figure 2. Equivalent two-degree-of-freedom model of proposed WEC.

2.3. Coupled analysis method of proposed WEC

From eqs. (1)-(3), it is clear that the vibration and circuit systems are strongly coupled through f_m , and Φ . Thus, a coupled analysis method is here introduced. First, a response surface of f_m and Φ is constructed. In short, sampling points of f_m and Φ are obtained by the finite element analysis in various combination of z , I_s , I_f . Then, those points are interpolated by a response surface, as which the RBF network is employed [9].

Using the response surface, we introduce the staggered method [10]. Namely, in each time step, (1), (2), (3) are solved alternatively until each unknown are converged. The flow of the coupled analysis is shown in Fig. 3. Let n and k denote the subscripts for the time step and sub-cycle, respectively. The solutions of (1), (2), and (3) for n -th time step are expressed as $z_{1,n}$, $z_{2,n}$, and I_n , respectively. In like manner, e.g., k -th sub-cycle solution is denoted by $z_{1,n,k}$. In each sub-cycle, the three equations are alternatively solved, and the solutions are updated. For example, the solution of (1) is updated as follows:

$$z_{1,n,k+1} = z_{1,n,k} + \alpha_k (\tilde{z}_{1,k} - z_{1,n,k}), \quad (4)$$

where $\alpha_k = \exp(-0.95k)$ is update coefficient, and $\tilde{z}_{1,k}$ is the temporally solution for k -th sub-cycle. Then, f_m and Φ are updated based on the k -th solutions. When all the solutions converge in the sub-cycle, e.g., $|z_{1,n,k+1} - z_{1,n,k}| < \varepsilon |z_{1,n-1}|$, the time-step is incremented.

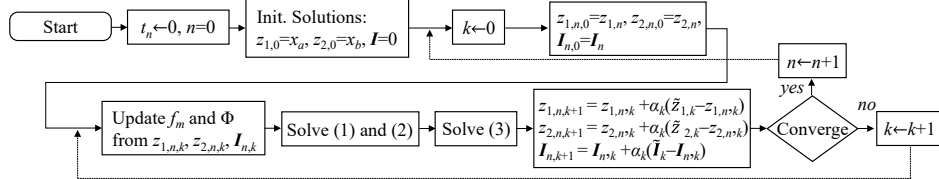


Figure 3. Basic flow of strong coupled analysis of proposed WEC.

3. Numerical Results

3.1. Target WEC model specifications

The detailed sizes of the proposed WEC considered in this work is shown in Fig. 4. The f_m and Φ for this model are analyzed by the finite element method with interval of $z = [-60\text{mm}, 60\text{mm}]$ in increments of 0.1mm for $I_s = 0\text{A}, +1\text{A}, -1\text{A}$ and $I_f = 0\text{A}, +1\text{A}, -1\text{A}$ respectively. To fit these points, the RBF network is learned, where about 5000 bases are uniformly located.

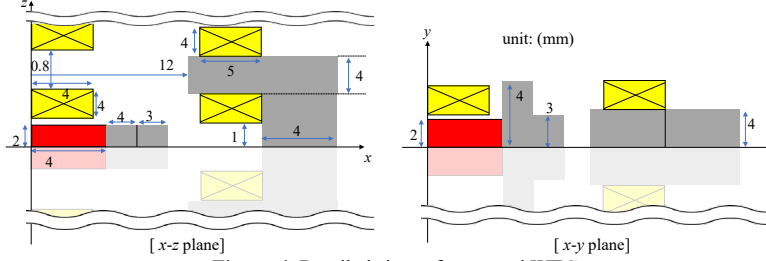


Figure 4. Detailed sizes of proposed WEC.

3.2. Potential energy design

The magnetic energy of the WEC model, $E_{\text{mag}}(z)$, is analyzed by FEM. By adding kinetic energies to $E_{\text{mag}}(z)$, the total potential energy, $E(z)$, is obtained as follows:

$$E(z) = E_{\text{mag}}(z) + \frac{1}{2}k_1z_1^2 + \frac{1}{2}k_2z_2^2 + \frac{1}{2}k_{12}(z_1 - z_2)^2. \quad (6)$$

In this work, to set the resonant frequency under 5Hz considering floating objects, k_1 is set to 10 Nm. Then, to form $E(z)$ as the double-well structure, k_2 , k_{12} are appropriately tuned. The potential energy structures for two different constants are shown in Fig. 5, from which we can see that $E(z)$ can become the double-well structure under the correct spring constants. Moreover, it can be seen that the proposed WEC becomes near to the linear system by setting larger spring constants. Here after, the spring constants set for Fig. 5(a) and Fig. 5(b) are respectively called “NL” and “L”, for simplicity.

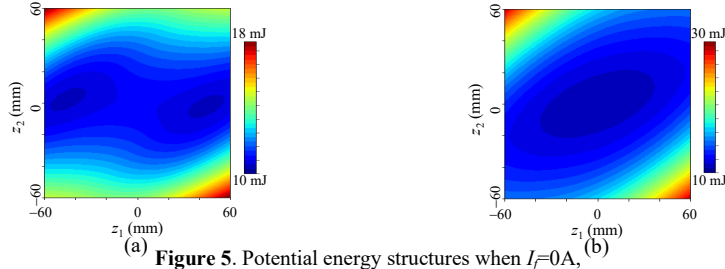


Figure 5. Potential energy structures when $I_f=0A$, (a): $k_1=10$ Nm, $k_2=200$ Nm, $k_{12}=50$ Nm, (b): $k_1=10$ Nm, $k_2=200$ Nm, $k_{12}=300$ Nm.

3.3. Simulation results

First of all, the frequency characteristics for no-load condition is analyzed under the condition that the input oscillation is set to 1G. The other parameters are summarized in Table I. In this condition, the original two resonant frequencies for the “NL” and “L” settings constants are (1.9Hz and 6.5Hz) and (2.8Hz and 9.9Hz), respectively. Hence, the frequency response from 0.5Hz to 12Hz is analyzed. The resultant frequency characteristics for “NL” and “L” settings are shown in Fig. 6(a). We can see that the “NL” setting has larger output especially when the input frequency is low, and “NL” has complicated frequency characteristic whereas “L” setting shows a simple 2-Dof characteristics. Moreover, the frequency characteristics when $I_f=1A$ is shown in Fig. 6(b).

It is shown that the frequency characteristic of “NL” can drastically be changed by I_f , while the characteristics for “L” is basically becomes larger because of the larger field magnetization. From these results, we can conclude that the proposed WEC can modify its frequency response by changing the field current depending on the vibrational input. Note that the operational range when $I_f=0A$ should be designed considering the basic wave condition. Then, the field current is sometimes inputted when the wave condition is temporally changed, e.g., bad weather, to minimize the electric energy for the field current. The time-variation of z and V for “NL” settings are shown in Fig. 7, which shows that the waveform is almost sinusoidal when the input frequency is near to the original resonant one. Otherwise, the waveform becomes complicated due to the nonlinearity. The too complicated voltage waveform in Fig. 7(a) is due to the large displacement; the magnets are far from the armature and the flux across the armature is not sinusoidal.

Second, the frequency characteristics when connecting a resistive load, R , are analyzed. The analysis settings are the same as the above-mentioned ones. The resultant frequency characteristics for three different R values are shown in Fig. 8, which shows that the output power dissipation in R for “NL” setting is larger than that for “L” settings. in wider frequency range. Note here that, from the impedance matching theory for

Table 1. Settings of analysis parameters

| Δt | inner resistance | m_1 | m_2 | c_1 | c_2 | c_{12} |
|------------|------------------|-------|-------|-----------|-------|----------|
| $T/100$ s | 20Ω | 350 g | 150 g | 0.15 Ns/m | | |

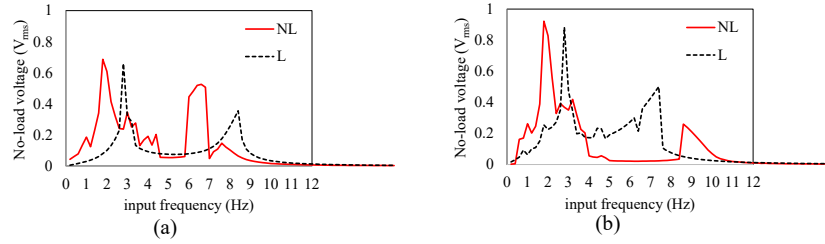


Figure 6. No-load voltage characteristic against input frequency. (a): $I_f=0A$, (b): $I_f=+1A$.

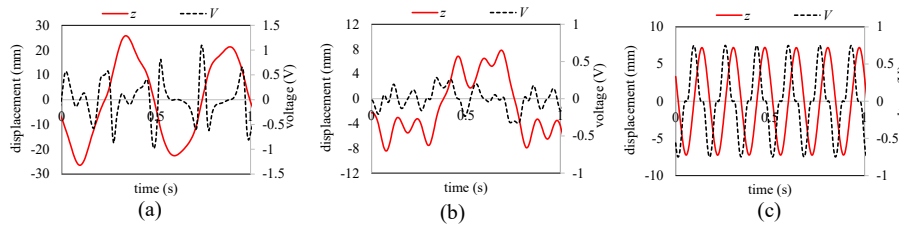


Figure 7. Time-variation of z and V for NL settings when $I_f=0A$. (a): 2Hz, (b): 3.5Hz, (c): 6Hz.

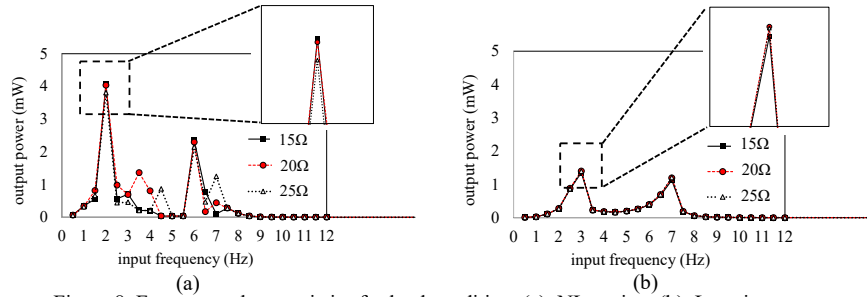


Figure 8. Frequency characteristics for load condition. (a): NL setting, (b): L setting.

electro-mechanical coupling [11], the maximum output should be obtained when R is a little larger than the inner resistance, 20Ω . In “L” setting, the output is maximized when R is about 20Ω , however, in “NL” setting, the maximum output is obtained when R is 15Ω . Moreover, it can be seen that the output characteristics vary by R in case of “NL” setting. This result indicates that the impedance matching theory for linear systems is not perfectly applicable for the nonlinear systems. A matching theory or suitable load circuits for the proposed nonlinear system is a remained problem.

4. Conclusion

The WEC with stochastic resonance and variable magnetization systems has been proposed. Moreover, the numerical analysis method for the proposed WEC has been introduced. From the numerical simulations, it has been shown that the proposed WEC has larger output especially when the input frequency is under 3Hz. In addition, the frequency characteristic can be changed by the field current.

For the future works, a prototype WEC will be manufactured, and the simulation results will be verified through the experiments.

Acknowledgements

This work was supported by JSPS KAKENHI Grant Numbers JP23K04247 and Nagamori Foundation’s research grant.

References

- [1] N. T. Mbungu, et. al., “An overview of renewable energy resources and grid integration for commercial building applications,” *Journal of Energy Storage*, vol. 27, Jun., 2020, Art. no 101385.
- [2] T. Wilberforce, Z. El Hassan, A. Durrant, J. Thompson, B. Soudan, “Overview of ocean power technology,” *Energy*, vol. 175, no. 15, pp. 165-181, May, 2019.
- [3] I. López, J. Andreu, S. Ceballos, I. M. Alegría, I. Kortabarria, “Review of wave energy technologies and the necessary power-equipment,” *Renewable and Sustainable Energy Reviews*, vol. 27, pp. 413-434, Nov., 2013.
- [4] R. Ahamed, K. McKee, I. Howard, “Advancements of wave energy converters based on power take off (PTO) systems: A review,” *Ocean Engineering*, vol. 204, no. 15, May 2020, art.id 107248.
- [5] A. V. Jaén, A. García-Santana, D. El Montoya-Andrade, “Maximizing output power of linear generators for wave energy conversion,” *International Transactions on Electrical Energy Systems*, vol. 24, no. 6, pp. 875-890, 2013
- [6] A. Pikovsky, M. Rosenblum, J. Kurths, R.C. Hilborn, “Synchronization: A Universal Concept in Nonlinear Science,” *American Journal of Physics*, vol. 70, no. 6, 2002.
- [7] R. L. Harne, K. W. Wang, “A review of the recent research on vibration energy harvesting via bistable systems,” *Smart Materials and Structures*, vol. 22, 2013, art no 023001.
- [8] Takahiro Sato, Hajime Igarashi, “A Chaotic Vibration Energy Harvester Using Magnetic Material,” *Smart Materials and Structures*, Vol. 24, No. 2, 2015, Art. no. 025033.
- [9] Y. Hidaka, “Mathematical-model-based Simulation Method for Wound Field Motors Using Alternative Flux Model by RBF-net,” *IEEJ Transactions on Industry Applications*, vol. 142, no. 8, pp. 609-619, 2022 (in Japanese).
- [10] T. Niho, et. al., “Numerical Instability of Magnetic Damping Problem of Elastic Plate,” *IEEE Trans. Magn.*, vol. 36, no. 4, pp. 1373-1376, 2000.
- [11] N.G. Stephen, “On energy harvesting from ambient vibration,” *Journal of Sound and Vibration*, vol. 293, no. 1-2, pp. 409-425, 2006.